

## CALIBRATIONS OF MULTI-HOLE PITOT TUBES DEPEND ON TUBULENCE

Iosif I. Shinder  
NIST  
100 Bureau Dr.  
Gaithersburg, MD  
20899-8361  
301-975-5943  
[ishinder@nist.gov](mailto:ishinder@nist.gov)

Christopher Crowley  
NIST  
100 Bureau Dr.  
Gaithersburg, MD  
20899-8361  
301-975-4648  
[chris.crowley@nist.gov](mailto:chris.crowley@nist.gov)

Michael R. Moldover  
NIST  
100 Bureau Dr.  
Gaithersburg, MD  
20899-8360  
301-975-2459  
[mmoldover@nist.gov](mailto:mmoldover@nist.gov)

***Abstract- NIST is developing techniques to calibrate 2- and 3-dimensional anemometer systems (such as multi-hole pitot tubes) with a resolution of 0.3 %. The pitch and yaw response of multi-hole pitot tubes is complicated; therefore, calibrations require hundreds of measurements. Until accurate models become available, NIST will disseminate the calibration data as tables. Many National Metrology Institutes (including NIST) calibrate anemometers in low-turbulence wind tunnels. During NIST's first calibration of a commercially manufactured multi-hole pitot tube, we observed hysteresis in the pressure differences between particular pairs of holes in particular ranges of airspeed, pitch angle, and yaw angle. In the worst case, the pressure difference for increasing air speed was 30 % larger than the pressure difference for decreasing air speed. By visualizing and mapping the flow near the pitot tube's surface, we demonstrated that this hysteresis was caused by boundary layer separation. The hysteresis disappeared when we added turbulence to the flow in NIST's wind tunnel.***

### Introduction

NIST is developing techniques to calibrate 2-D and 3-D anemometer systems, including multi-hole pitot tubes. One motivation for this project is an emerging need to measure the CO<sub>2</sub> flux (the product of flow rate and CO<sub>2</sub> concentration) in the stack gases emitted by coal-burning power plants with uncertainties on the order of 1%. In 2010, eastern Canada and the northeastern states of the United States agreed to the Regional Greenhouse Gas Initiative (RGGI). This initiative aims to reduce CO<sub>2</sub> emission by 10% by 2018. This goal implies a need for accurate CO<sub>2</sub> flux measurements. Today, CO<sub>2</sub> flux measurements are made in stacks to control the emissions of the pollutants SO<sub>2</sub>, NO<sub>x</sub> and Hg; however, present-day CO<sub>2</sub> flux measurements may have uncertainties in the range 5 % to 10 %. [1, 2] Reducing these uncertainties may require 2-D or 3-D probes to account for the large swirl that occurs in many power plant stacks. Furthermore, new calibration techniques may be required to calibrate 2-D and 3-D instruments.

One of the most widely used methods for measuring the efflux of greenhouse gasses is pitot tube survey of the stack cross-section. The EPA has developed protocols for stack surveys using 1, 2 and 3 dimension static differential pressure devices, such as regular pitot static tubes, S-probes and multi-hole pitot tubes. NIST has designed and installed a manual rig for calibrating 2-D and 3-D airspeed instruments. In the near future an automated rig will replace the manual one. NIST's first calibration of a five-hole conically-shaped pitot tube revealed a flow instability that introduced hysteresis into the calibration data. This hysteresis was removed when turbulence was introduced into the flow. We plan to study the turbulence-dependence of air-speed calibrations. We anticipate that NIST's low-turbulence wind tunnel will be modified to calibrate pitot tubes used to survey turbulent flows in stacks.

### Multi-hole static pitot tube.

Multi-holed, or 3-D, pitot tubes are used to measure a fluid's velocity, in situations where a 1-D pitot tube cannot be accurately aligned with the flow. Multi-holed pitot tubes determine the velocity, yaw angle, and pitch angle from measurements of the differential pressure between pairs of holes located near the tip of

the sensor [3]. The Environmental Protection Agency (EPA) has approved measurement protocols that use multi-holed pitot tubes to determine the flux of greenhouse gasses and other pollutants emitted into the atmosphere from smokestacks for regulatory purposes. The protocols require measurements of the gas's composition and flow from a stack. The flow is determined by integrating velocity measurements made by traversing a velocity sensor, such as a multi-holed pitot tube, along diametric chords of the stack. This method of measuring flux is traceable to SI units through the calibration of the pitot tube. NIST is developing techniques to calibrate 2-D and 3-D airspeed anemometer systems, including multi-hole pitot tubes. The pitch and yaw response of multi-hole pitot tubes is quite complicated; therefore, accurate calibrations require thousands of measured points. Because we lack accurate models, the calibration data is disseminated as tables instead of using calibration factors related to dynamic pressure as is done for standard pitot tubes and S-probes.



**FIGURE 1. Manual 3-D calibration rig.**

## Airspeed calibration facility

NIST's Dual Test Section Wind Tunnel is a toroid-shaped, closed-loop structure lying in a horizontal plane [4, 5]. The wind tunnel has two interchangeable test sections in order to span the range of airspeeds from 0.2 m/s to 75 m/s. Both test sections are 12 m long; however, their cross-sections differ. The low-speed test section is used for calibrations ranging from 0.2 m/s to 45 m/s and it is 2.1 m high and 1.5 m wide. The high-speed test section is used for airspeed calibrations up to 75 m/s. Its height gradually decreases from 2.1 m to 1.2 m along the flow direction, forming a venturi-like duct. Both test sections provide longitudinal free-stream turbulence levels of 0.07 % over most of the airspeed range and a transverse velocity gradient of less than 1% within a working area that spans 90% of the test section's areas.

## Calibration rig

The present research used the manually operated calibration rig shown in Fig. 1. This rig was attached to the wall of the high-speed section of the wind tunnel. The pitch angle between the pitot tube and the flow was varied by rotating the instrument under test (IUT) along the aluminum shelf. The yaw angle was varied by rotating the IUT inside the mounting clamps. The flat aluminum plate supported the IUT and was marked to measure pitch angles. The yaw angle was measured by a digital inclinometer coupled to the IUT. The uncertainty of yaw and pitch measurements were  $0.1^\circ$  and  $0.2^\circ$  respectively. This calibration rig can be used to calibrate any 3-D anemometer that can be mounted on a rod.



**Figure 2. Cone-shaped, five-hole pitot tube. The diameter of the curved tube was 9.5 mm.**

We are developing a new, automated calibration rig. It will have four degrees of freedom in order to ensure the sensor tip is always at the same location in the wind tunnel. To ensure circular movement about the sensor tip, two linear and two rotational traversers will be used.

## Unexpected finding: hysteresis

During a calibration of the cone-shaped, five-hole pitot tube<sup>1</sup> shown in Fig. 2, we discovered that when the tube was oriented in the range  $20^\circ \pm 5^\circ$  away from the tunnel's axis, strong hysteresis was present in the measured values of pressure differences as the air speed was increased and decreased. (See Fig. 3, top.)

To characterize the hysteresis we defined the calibration factor  $C_i$  by the ratio

$$C_i \equiv \Delta P_{\text{IUT},i} / \Delta P_{\text{standard}}$$

The numerator of  $C_i$  is the pressure difference between the center hole and the  $i^{\text{th}}$  off-axis hole of the instrument under test (IUT). The denominator of  $C_i$  is the differential pressure measured by a 1-D pitot tube that NIST routinely uses as a check-standard for measurements of air speed. The check standard was located one meter away from the IUT and in the same cross sectional plane of the wind tunnel.

As shown in Fig. 3,  $\Delta P_{\text{IUT}}$  was smaller when the air speed increased than when the air speed decreased. By exchanging the differential pressure sensors and associated instruments, we verified that the hysteresis did not originate in the instruments. Instead, the hysteresis resulted from the flow interacting with the pitot tube itself. Because the sensing region of the pitot tubes is small, we decided to study the flow around the pitot tube using a fully-functional, scale-model tube that was a factor of 5 larger than the commercially manufactured pitot tube. To match Reynolds numbers, the velocity range was reduced by a factor of 5. As shown in the lower panel of Fig. 3, the model tube and the “real” tube had hysteresis of comparable size at comparable yaw angles at velocities consistent with Reynolds  $1/5^{\text{th}}$  scaling. The hysteresis in the model was approximately 10% while the hysteresis in the original tube was approximately 17%. Perhaps this difference resulted from errors in machining the scaled model.



Figure 4. Visualization setup.

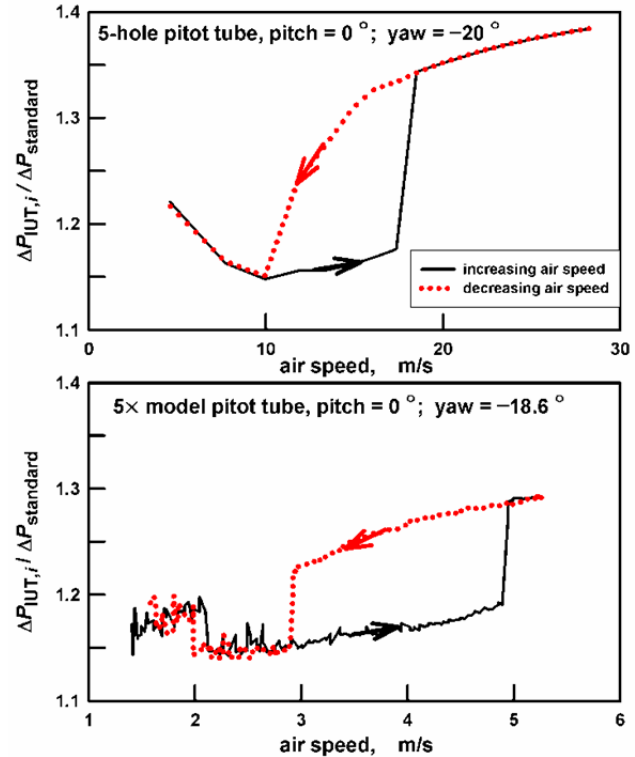
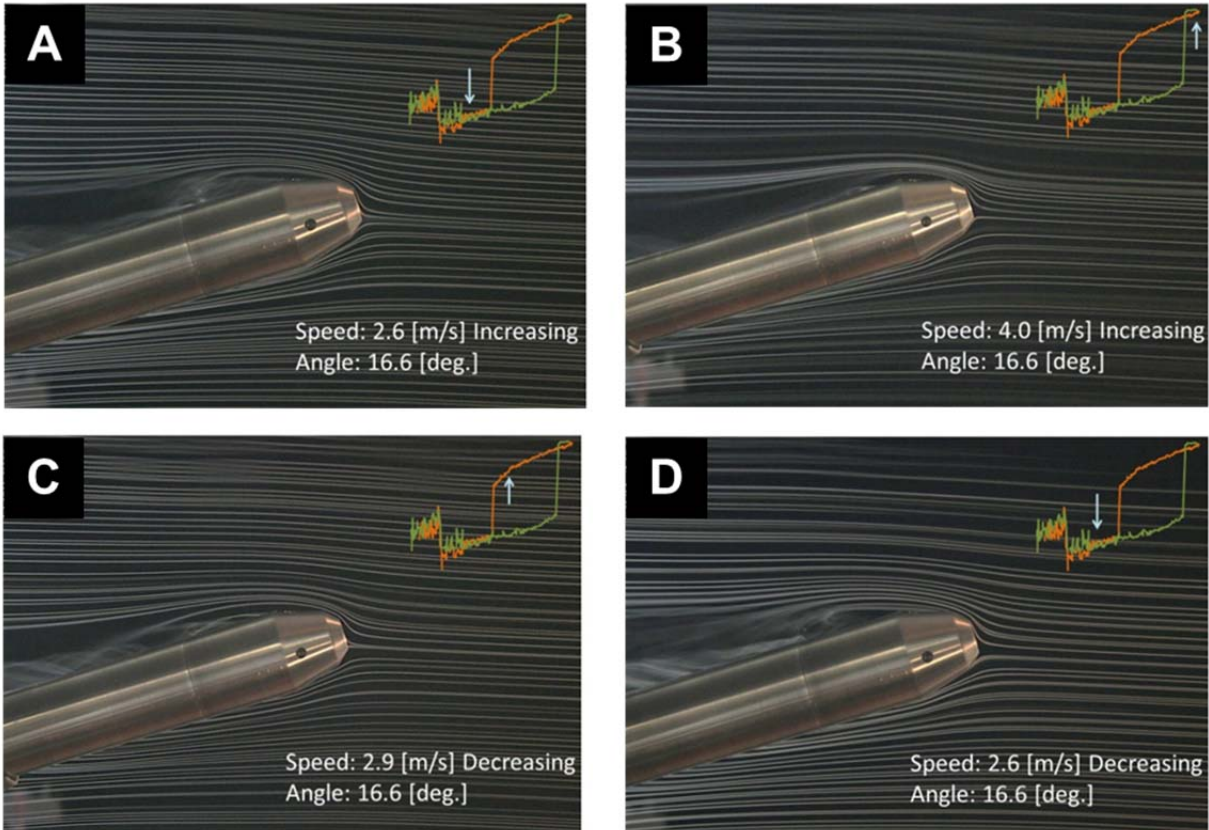


Figure 3. Hysteresis in pressure differences for the commercially-manufactured pitot tube and the five-times-larger model occur at similar Reynolds numbers.

## Visualization

Figure 4 shows the setup used to generate smoke streamlines that visualized the flow around the 5X model pitot tube. A 0.25 mm diameter nickel-chromium wire was installed upstream of the pitot tube. The wire's diameter was so small that it did

<sup>1</sup> Model DC-250-78.72-J-76.72-CD manufactured by United Sensor Corp., Amherst, N.H. USA. In order to describe materials and procedures adequately, it is occasionally necessary to identify commercial products by manufacturer's name or label. In no instance does such identification imply endorsement by the National Institute of Standards and Technology, nor does it imply that the particular product or equipment is necessarily the best available for the purpose.



**Figure 5. Visualization of flow around model pitot tube. Note strong recirculation in A and D.**

not disturb the flow. Upon command from outside the wind tunnel, a capillary tube dropped “ProtoSmoke<sup>1</sup> fluid” (toy model train smoke oil) near the top of the wire. The oil naturally ran down the wire and beaded up into droplets that became smoke streaks when a current was passed through the wire. To enhance contrast, a black cloth was attached to the wall of the tunnel opposite the camera and back lighting was applied from either side of the black cloth. Representative pictures are shown in Fig. 7. The photographs revealed a recirculation zone above the hole that exhibited hysteresis correspond to the differential pressure measurement. All four pictures in Fig. 7 show flow separation; however pictures (A) and (D) have a noticeably more turbulent recirculation zone. Based on the pictures, the portion of the calibration curve that is discontinuous appears to be linked to the flow separation. With the information gained from the photographs, we began a more quantitative investigation.

### **LDA survey near the pitot tip.**

We used a laser-Doppler anemometer to measure the 3-D velocity profile near the tip of the 5X<sub>x</sub> model. Here, we discuss only the tangential flow velocity measured approximately 0.03 mm above the pitot tube’s surface. As shown in Fig. 6, the tangential velocity has hysteresis in the same range of airspeeds that the differential pressure has hysteresis. Note that the tangential air flow above the surface near the hole is in the direction opposite to the primary flow generated by the tunnel. As the airspeed in the wind tunnel increases, the magnitude of counter-flow slowly increases. At a particular airspeed (4.5 m/s in Fig.6, the flow detaches from the pitot tube’s surface. Once detached, the magnitude of the counter-flow is approximately 85% of the air speed in the wind tunnel. When the air speed is decrease, the flow gradually re-attaches to the pitot tube at a lower air speeds than the detachment at 4.5 m/s. This is typical of boundary layer separation.



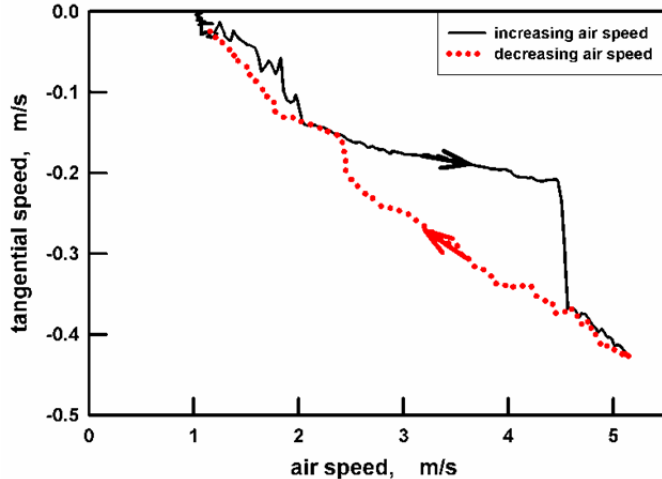


Figure 6. Tangential air speed 0.03 mm above the surface of the 5X model pitot tube.

To test the role, if any, played by the holes themselves, we rotated the 5× model by 45°, thereby moving the hole out of the recirculation zone. The counter-flow velocity exhibited the same behavior; therefore, the hysteresis was not caused by the holes but, by the geometry of the pitot tube itself.

## Turbulence removes hysteresis

We emphasize that boundaries of the hysteresis are not well defined; a small vibration or change in the angles causes the flow to go from less stable state (black lines in Figs. 3 and 6), to a more stable state (red lines in Figs. 3 and 6). NIST's wind tunnel was designed to produce very quiet flows. The level of turbulence over its whole

operating range does not exceed 0.07%. To demonstrate that turbulence suppresses hysteresis, we installed a wooden grid 6 m upstream of the pitot tube, before a contraction in the cross-section of the wind tunnel. The size of the grid cell is 10 cm. Fig. 7 shows that the grid eliminated the hysteresis. In the presence of turbulence, the curves corresponding to increasing and decreasing of the airspeed coincide.

## Summary

Detached flow can produce a very strong hysteresis in a velocity sensor at certain pitch and yaw angles. Calibration of the multi-hole pitot tube should be performed at a certain level of turbulence. In real stacks the hysteresis will not be observed due to the high level of turbulence. But even in the case of stack measurements it is possible that the calibration factor will depend of level of turbulence. We are planning to perform a special research in order to find out the dependence of the calibration factor on turbulence.

## References

- [1] Marland, G.; Rotty, R.M. Carbon Dioxide emissions from fossil-fuels: A procedure for estimation and results for 1950-1982. *Tellus, Ser B*: 1984, 36, 232-261.
- [2] U.S. Energy Information Administration. Documentation for Emissions of Greenhouse Gases in the United States 2005; EIA: Washington D.C., 2007
- [3] D. W. Bryer, R. C. Pankhurst, Pressure-probe methods for determining wind speed and flow direction, 1971.
- [4] T.T. Yeh, M.J. Hall. *Airspeed Calibration Service*. NIST Special Publication SP 250-73.
- [5] I.I. Shinder, M.J. Hall, M.R. Moldover. Improved NIST Airspeed Calibration Facility. Proceeding of the MSC 2012, Pasadena, California.

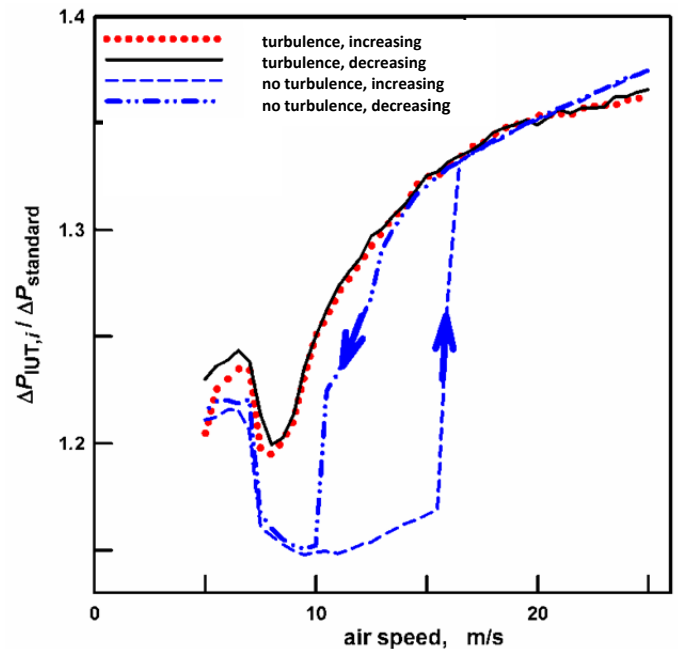


Figure 7. Comparison of differential pressure data with and without turbulence.